HHS Public Access

Author manuscript

Pain. Author manuscript; available in PMC 2024 February 01.

Published in final edited form as:

Pain. 2023 February 01; 164(2): 280–291. doi:10.1097/j.pain.0000000000002731.

Disentangling self from pain: mindfulness meditation-induced pain relief is driven by thalamic-default mode network decoupling

Gabriel Riegner[1], **Grace Posey**[2], **Valeria Oliva**[1], **Youngkyoo Jung**[3], **William Mobley**[4], **Fadel Zeidan**[1,*]

[1]Department of Anesthesiology; University of California San Diego; La Jolla, CA, 92037; United States

[2]Department of Medicine; Tulane University School of Medicine; New Orleans, LA, 70112; United States

[3]Department of Radiology; University of California Davis; Sacramento, CA, 95817; United States

[4]Department of Neurosciences; University of California San Diego; La Jolla, CA, 92093; United States

INTRODUCTION

Pain is constructed and modulated by a dynamic interplay between real-time appraisals of corresponding sensory, cognitive, and affective processes. Mindfulness meditation, a self-regulatory technique, is highly effective at reducing self-reported experimental and chronic pain [7; 9; 15; 38]. It is practiced by promoting a “detached observation” to reduce the self-referential value of all arising sensations. Mindfulness meditation is more effective and engages distinct neural [51], endogenous [26; 45], and parasympathetic [1] mechanisms from placebo to reduce pain. Using perfusion-based functional magnetic resonance imaging (fMRI) acquisition, we found that meditation-induced pain reductions were directly associated with higher cerebral blood flow (CBF) in the ventrolateral prefrontal (vlPFC)/orbitofrontal (OFC) cortex and lower CBF in the contralateral thalamus [51; 52]. Based on these reproducible effects, we proposed that mindfulness meditation-induced pain relief would be driven by unique cortico-thalamocortical nociceptive filtering mechanisms reflected by a) stronger connectivity between the right OFC and contralateral thalamus to reflect excitatory innervations on the inhibitory thalamic reticular nuclei (TRN),

*Correspondence: fzeidan@ucsd.edu.

AUTHOR CONTRIBUTIONS

G.R. and V.O. were involved in conceptualization, data curation, formal analysis, methodology, visualization, writing - review & editing.

G.P. was involved in conceptualization, investigation, project administration.

J.Y. was involved in data curation, investigation, methodology.

W.M. was involved in writing – review & editing.

F.Z. was involved in conceptualization, data curation, formal analysis, funding acquisition, methodology, project administration, resources, supervision, validation, writing - original draft.

DECLARATION OF INTERESTS

The authors declare no competing interests.

and b) weaker contralateral thalamus - primary somatosensory cortex (S1) connectivity, respectively. However, previous work employing perfusion fMRI [51; 52] were not optimized to dissect event-related functional connectivity because of low temporal resolution (repetition times > 9 seconds). Thus, there are no known studies that have identified the functional connections supporting the direct attenuation of pain by mindfulness meditation.

Growing evidence [10; 53] also indicate a relationship between mindfulness meditation-related health benefits and attenuated default mode network processing. The default mode network is characterized by oscillating activity between the medial prefrontal cortex (mPFC), posterior cingulate cortex (PCC)/precuneus, inferior and lateral temporal cortices. The default mode network is critically involved in facilitating self-referential processes [36; 39] and pain-related ruminations [3; 24]. Higher self-reported trait mindfulness was associated with lower pain sensitivity and weaker processing in the PCC/precuneus during noxious heat stimulation in meditation naïve individuals [21; 55]. However, the brain mechanisms supporting trait mindfulness are different from those engaged by the *active* practice of mindfulness meditation in response to pain-evoking stimulation. Thus, the proposed work extends upon prior investigations by examining the neural connectivity explicitly engaged by mindfulness meditation during noxious stimulation to reduce pain.

The proposed preregistered mechanistically focused clinical trial (NCT03414138) combined blood oxygen level dependent (BOLD) signaled fMRI acquisition with psychophysical pain testing [49°C stimulation & pain-focused visual analog scales (VAS)] to identify the neural connectivity supporting the direct modulation of pain-related behavioral and neural responses by mindfulness meditation. We postulated that mindfulness meditation reduces pain by eliciting a prefrontal mediated nociceptive gating mechanism at the level of the thalamus. Separate 2 (mindfulness vs. control group) X 2 (pre-rest) vs. post-mindfulness/rest) general linear model (GLM) analysis of variance (ANOVA) examined if mindfulness meditation produced significant reductions in behavioral and neural pain responses when compared to the controls. All neuroimaging analyses were conducted during pain-evoking 49°C heat to identify brain mechanisms supporting the *direct attenuation* of pain by mindfulness meditation. Based on updated working hypotheses and to test the primary of the study, whole-brain and seed-to-seed psychophysiological interaction analyses (PPI) [33] were performed to determine if mindfulness meditation-induced pain relief would be moderated by a) stronger lateral OFC connectivity with the contralateral thalamus and b) weaker thalamic connectivity with the SI representation of the noxious stimulation site (right calf). The present findings provide novel evidence that the direct modulation of pain by mindfulness meditation is moderated by brain mechanisms supporting the attenuation of self-referential and nociceptive processing.

METHODS

Sample Size Determination

Based on previous work [50; 51], we expected a large behavioral and neural effect size difference between mindfulness meditation and non-manipulated controls. Our prior fMRI-based contrast of parameter estimates (COPE) [left thalamus; right OFC] [52] and fMRI-based statistical power calculating software (fmripower.org) were used to calculate sample

size determination. Forty participants (n = 20/group) provided over 85% statistical power to detect the hypothesized large-effect sizes (r = .50) exhibited in predefined [52] brain mechanisms supporting meditation-induced pain reductions.

Participants

Wake Forest School of Medicine's Institutional Review Board approved (IRB#182082) all study procedures. One hundred and thirty-seven healthy, pain-free, and meditation-naive participants (18–65 years of age) were screened from the local community. Exclusion criteria included individuals that were claustrophobic, pregnant, and/or had MRI contraindications. All participants provided written informed consent at the initial study visit with all methods clearly explained, acknowledging that 1) they would experience painful heat stimuli, and 2) they were free to withdraw from the study at any time.

At screening, 79 participants were excluded for not meeting inclusion-exclusion criteria (Figure 1). Fifty-eight participants were enrolled in the study, but 18 individuals did not complete study procedures for several reasons (Figure 1). Forty participants (all right-handed; mean age = 30 years ± 10 years; 20 males; 20 females) were included in the final analysis (22 = White, 13 = Black, 3 = Hispanic, 1 = Asian, and 1 = Native American; Figure 1).

Randomization Procedure

Group randomization was stratified by sex (10/group) after successfully completing session 1 (Figure 2). Males and females were randomized without replacement using a random number generator by a research technician not involved in data collection. Participants were informed of their respective group assignments after session 1.

Stimuli

An fMRI-compatible thermal sensory analyzer (TSA-II, Medoc, Inc., Raleigh, NC) fitted with a 16mm^2 surface area probe delivered all thermal stimuli. Heat series during the experiment (300s duration) consisted of ten alternating 10s plateaus of 49°C interleaved with 14 second 35°C stimulation delivered to the back of the right calf. To minimize habituation, the thermal probe was moved to a new stimulation site on the right calf after each experimental series. Participants were free to remove the stimuli at any time by lifting their limb away from the probe-holder.

Psychophysical Assessment of Pain

Pain intensity and unpleasantness ratings were assessed with a 15cm sliding visual analog scale (VAS). The minimum rating (0) was designated as "no pain sensation" and "not at all unpleasant" whereas the maximum (10) was labeled as "most intense pain sensation imaginable" or "most unpleasant sensation imaginable", respectively. Participants were instructed to use the VAS scale only if they felt the stimulus to be painful. Thus, if there was no pain to report, participants verbalized with a "0" or "no pain".

Anatomical MRI Acquisition

MRI data were acquired on a 3T Siemens MAGNETOM Skyra scanner with a 32-channel head coil (Siemens Healthineers AG, Munich, Germany). High-resolution structural scans were acquired using an MP-RAGE sequence [TI= 900 milliseconds (ms); TR= 2300ms; flip angle= 9°; TE= 2.98ms; 1mm isotropic spatial resolution; 192 slices, GRAPPA factor = 2; scan time = 312 seconds (s)].

Functional MRI Acquisition

For functional imaging, blood-oxygen-level-dependent (BOLD) images were acquired using echo-planar imaging (EPI; TE = 25ms; TR = 2000ms; 35 × 4-mm-thick slices with no gap; 4.00 × 4.00 mm in-plane resolution; flip angle= 75°; 180 repetitions; scan time = 300s).

Experimental Design

Experimental Session 1 (Psychophysical Training + Baseline Pain Testing)— After providing written consent, participants were 1) familiarized with 32, 5s duration thermal stimuli (35 – 49°C) on the ventral aspect of the forearm and 2) trained to use the pain VAS. Afterward, participants placed their right calf on a custom-made thermal probe holder. Baseline psychophysical pain responses were assessed in response to noxious heat by administering a total of four *heat* series. VAS pain intensity and unpleasantness ratings were collected after each series, and the thermal probe was moved to a different region on the back of the right calf. Throughout session 1 (Figure 2), participants were instructed to remain still and sit quietly. After the first two heat series, participants were told to continue to "sit quietly" for 10 minutes to control for the time elapsed in the post-intervention MRI session. Following, two heat series were administered, and pain ratings were collected, respectively. After successful completion of sensory testing, participants were randomized to one of groups and informed of their respective group assignments.

Experimental Session 2–5 (Intervention Sessions)

Mindfulness Meditation Training Regimen: As adapted in our previous work [1; 45; 52], participants in the mindfulness meditation group participated in four separate sessions (20 minutes each and on separate days) of mindfulness-based mental training. These sessions were facilitated by experienced mindfulness instructors. Across all the meditation training sessions, participants were instructed to focus on the changing sensations of the breath and to reduce self-referential judgments by acknowledging arising thoughts, feelings, and emotions without judgment or emotional reaction. When attention to breathing sensations disengaged, participants were encouraged to "simply return their attention back to the breath sensations". Participants were instructed not to explicitly change their breathing rate. Contrary to traditional meditation training interventions, participants were explicitly instructed to not practice meditation outside of study training to reduce inter-individual variability in practice time effects. In meditation training session 3, the same basic principles of the previous sessions were reiterated. An audio recording of fMRI scanner sounds was introduced during the last 10 minutes of meditation training to familiarize participants with meditating in an MRI environment. On the final training session (session 4), participants

received minimal meditation instruction and were required to lie in the supine position and meditate during an audio recording of the fMRI sounds to simulate the scanner environment.

Book Listening Control Regimen: The control group listened to an audio recording of *The Natural History and Antiquities of Selborne* across four sessions (20 minutes each and on separate days). This book has been used a neutral comparison regimen in our studies because it does not improve mood but controls for the time elapsed in the meditation intervention, facilitator attention, and a group session, respectively [50]. Audio recordings continued serially from where they ended in the previous book-listening session. Therefore, participants who successfully completed the book-listening regimen listened, in total, to 80 minutes of the *Natural History and Antiquities of Selborne*. Study volunteers were not allowed to sleep, use their phones, or talk to the experimenter during book listening. In control session 3, we introduced the sounds of the scanner in the last 10 minutes of book listening. To better match the procedures to the meditation group, participants were instructed to lie in the supine position and listen to the audiobook and sounds of the scanner during book listening session 4.

Experimental Session 7 (Functional MRI)—Participants first reported to the Wake Forest Center for Biomolecular Imaging and were positioned in the MRI scanner with a respiratory transducer around the chest and a pulse oximeter on the left index finger (respiration and heart rate data not presented here). Participants positioned their right calf on a custom-made thermal probe holder fitted with a force transducer to continuously confirm contact of the thermal probe with the calf. All physiological and thermal heat stimuli were logged with a digital chart recorder (MP160, Biopac Systems Inc.).

Pre-Manipulation—During the pre-manipulation condition (characterized as “rest”), all participants were instructed to “not move” and keep their “eyes closed”. There were two types of thermal stimulation series: 1) Heat series (300 second (s) duration) = ten alternating 10s plateaus of 49°C and 14 seconds of 35°C stimulation, and 2) Neutral series (300s duration; neutral series not presented here) = continual 35°C stimulation. Participants were administered 2 *neutral* (not presented here) and 2 *heat* series, to the back of the right calf, in an alternating fashion and pain ratings were collected after each series.

An anatomical scan was then collected after participants in the mindfulness meditation group were instructed to “begin meditating and to continue until the end of the experiment”. As in our prior meditation-fMRI studies [51; 52], we provided meditation group participants supplementary time during the anatomical acquisition to establish a meditative state before functional acquisition. Members of the control group were instructed to continue to “lie still with your eyes closed” and to not move. After the structural scan, participants were provided three supplemental minutes in silence before continuing fMRI acquisition and heat stimulation.

Post-Manipulation—Participants were administered alternating series of 2 *neutral* (not presented here) and 2 *heat* series during the post-manipulation scan. Post-manipulation is characterized as “control-rest” for the control group and “meditation” for the mindfulness meditation group. Pain ratings were collected after each heat series.

Analysis of Behavioral Data

A 2 manipulation (pre vs. post) X pain type (intensity vs. unpleasantness) X group (mindfulness vs. control) X session (1 & 6) ANOVA tested (SPSS v27, IBM, Armonk, New York) the primary hypothesis that mindfulness meditation would produce greater pain reductions than rest and the book-listening control group. Significant main effects and interactions ($p < .05$) were investigated with planned simple effects tests.

Analysis of Neuroimaging Data

All neuroimaging data were analyzed using FSL version 6.00 employing customized analytical methods.

Preprocessing—Six seconds of non-steady 4D data were removed from the start of each functional acquisition. To correct for B0 field non-uniformity, fieldmap unwarping was applied (FSL FUGUE). Distortion corrected functional images were co-registered to their corresponding T1w reference using FLIRT boundary-based registration, the standard MNI template through 12-parameter linear, and 10mm warp resolution nonlinear transformations. Head-motion was corrected and the analogous six rotation and translation parameters were estimated. From these motion parameters, framewise displacement was calculated and used to flag motion outliers above 0.9mm displacement. Functional images were then spatially smoothed using a gaussian kernel (full-width half-maximum of 5mm), and high-pass filtered with a period of 100s. Autocorrelation correction and model estimation was applied using FILM.

White matter (WM) segmentation was performed for each structural T1 (FSL FAST), thresholded at 99% probability then eroded, before being registered to each respective functional image. A timeseries (eigenvariate) was extracted from each subject's WM mask to regress out non-neural sources of noise.

General Linear Model—For the four fMRI-based noxious *heat* series, the general linear model (GLM) design matrix included a stimulus regressor indicating the onsets and durations of the ten, 10 heat stimuli (a total of 100s of noxious 49°C) relative to an implicit baseline (a total of 180s of innocuous 35°C). This regressor was scaled to +1, temporally filtered, and convolved with a double gamma model of the hemodynamic response function; and its temporal derivative was added to the model. Each model also included covariates of no interest – a high-variance signal from WM, 6 head motion parameters, and separate regressors for each volume flagged as high motion, to reduce physiological and motion-related noise. The results of this GLM were effect size (β) maps of the stimulus-related regional signal changes.

We performed intra-subject fixed effects (second level) analyses within each subject separately for the stimulus regressor and proceeded to inter-subject mixed effects (third level) analysis using a whole-brain between-group independent samples t-test on the contrast maps of pre (rest) vs. post manipulation (meditation or rest). Within each group demeaned and residualized (pre-rest vs. post-manipulation) pain intensity and unpleasantness (orthogonalized to intensity) ratings were entered as covariates to determine whole-brain

voxel-wise correlations with changes in pain intensity. Importantly, Z (Gaussianized T/F) statistic images were determined using FLAME 1+2 and a corrected cluster of height z ± 3.10 and size p < 0.05, controlling for family-wise error rate [12].

Seed-to-seed and Whole-Brain Psychophysiological Interaction Analyses— To directly test our working hypotheses, we conducted two, seed-to-seed and two seed to whole-brain PPI analyses to investigate heat stimulus-modulated connectivity [33] comparing pre (rest) and post-manipulation (meditation or rest). Within each group we tested pre-registered connections of interest— a) left thalamic to whole-brain, b) right OFC to whole-brain, c) right OFC -> left thalamus, and d) left thalamus -> left SI representation of the stimulation site on the right calf.

Seed regions were created from the Higher Order Dictionaries of Functional Modes-128 component (DIFUMO) atlas [11]. Seeds were selected from the contralateral left thalamus and right OFC that overlapped with the peak voxel coordinates of brain mechanisms supporting meditation-related analgesia in a previous study [52]. A seed corresponding to the left lateralized SI representation of the right leg was manually created using a 5mm mask around the right calf representation [2] that overlapped with the coordinates corresponding to peak right calf activation from our previous study [52]. The standard space of these seed regions were linearly transformed to each functional image, then binarized at 75% probability, and the eignenvariate values were extracted.

PPI models were generated for each heat series employing three regressors. The first regressor (psychological regressor) modeled the zero-centered convolved heat stimulus (see General Linear Model), the second regressor (physiological regressor) was the mean-centered time series values from the seeds (respectively), and the third regressor was the interaction regression term between the first (psychological) and second (physiological) regressors. Denoising covariates paralleled those of the GLM described above. Within each subject, we then compared pre (rest) vs. post (meditation) manipulation PPI connectivity during 49°C as compared to 35°C. The contrast maps of these second level analyses were entered into third level within group analyses. Further, demeaned residuals (post – pre-manipulation) of pain intensity and unpleasantness (orthogonalized to intensity) ratings were entered as covariates. All whole-brain PPI analyses accounted for mixed effects (FLAME 1+2) and were thresholded using a corrected cluster of height z ± 3.1 and size $p < .05$, controlling the family-wise error rate [12; 46]. Seed-to-seed tests restricted the analysis space to a priori regions of interest using non-parametric permutation testing (FSL RANDOMISE). Statistical inferences were based on Threshold-Free Cluster Enhancement, $p < .05$ [40].

RESULTS

Behavioral Findings

Mindfulness meditation significantly reduced pain—There were no significant between-group differences in pre-intervention pain ratings, $F(1, 34) = .11$, $p = .75$, $\eta^2_p = .03$ (Figure 3). The RM ANOVA revealed a significant group X manipulation X session interaction, $F(1, 38) = 18.59$, $p < .001$, $\eta^2_p = .33$. To interpret the significant interaction,

simple effects tests determined that mindfulness meditation produced significant reductions in pain intensity (−32%) and pain unpleasantness (−33%) ratings from rest to meditation and when compared to pre to post-manipulation in the control group, respectively (*ps* <.001; Figure 4). In the post-intervention MRI session, the control group reported significantly higher pain from pre (1st half of scan) to post-manipulation (2nd half of scan; p =.05). As expected, both groups reported lower pain in the pre-manipulation session 6 when compared to pre-manipulation in session 1. Yet, the controls exhibited significant pain habituation [48] from session 1 to 6 (*p* =.003) and when compared to the meditation group (*p* = .004) during pre-manipulation. The pain habituation effect is perplexing but may be associated with relief that the experiment was almost over.

Neuroimaging Findings

Mindfulness Meditation-Induced Pain Relief is Associated with greater vmPFC Deactivation—Importantly, statistical power calculation analyses (NCT03414138) successfully predicted this study's large behavioral and brain-based effect sizes. All analyses were conducted during noxious heat stimulation (49°C). A whole-brain independent samples t-test found that mindfulness meditation produced significant reductions in nociceptive processing regions including the bilateral posterior insula, secondary somatosensory cortices (SII), parietal operculum, dorsal ACC (dACC), supplementary motor area (SMA), and cerebellum during noxious heat stimulation (Table 1; Table 2; Figure 5 left panel) when compared to rest and from pre to post-manipulation in the control group, respectively.

During noxious heat, the within-group ANOVA established that mindfulness meditation reduced bilateral amygdala, hippocampus, and mid and anterior insula activation when compared to rest (Figure 5 middle panel). Importantly, greater mindfulness meditation based pain reductions were, from rest to meditation, associated with greater vmPFC deactivation (Figure 5 right panel). The control group exhibited greater occipital lobe activation in the second half of the scan when compared to the first half of the scan (Figure 6).

Mindfulness Meditation-Induced Pain Relief is Moderated by Weaker Thalamic-Precuneus Connectivity—Contralateral thalamic-whole-brain PPI analyses revealed that greater meditation-induced reductions, from rest to meditation, in pain intensity ratings were associated with greater thalamic decoupling from the precuneus and the primary visual cortex (V1) (Figure 7). There were no other significant meditation-related mean effects, correlations, or control group effects.

Mindfulness meditation reduces pain by attenuating PFC-thalamic and thalamic-SI connectivity—Contrary to our hypotheses, seed-to-seed PPI analyses indicated that weaker right OFC connectivity with the contralateral thalamus predicted mindfulness meditation induced reductions in pain from rest to meditation (Figure 8 top panel). However, as predicted, weaker thalamic-SI functional connectivity predicted stronger meditation-induced pain intensity reductions (Figure 8 bottom panel).

Mindfulness Meditation-Induced Pain Relief is Moderated by Weaker OFC-posterior insula/SII Connectivity—Right-OFC to whole-brain PPI analyses revealed

that greater meditation-induced pain relief, from rest to meditation, was associated with weaker OFC connectivity with the contralateral posterior insula, SII and parietal operculum (Figure 9). There were no other significant meditation-related mean effects, correlations, or control group effects.

DISCUSSION

The dynamic transformation of nociceptive information into a subjectively available pain experience is predicated on intrinsically reflexive interpretations of ascending noxious input. In contrast, mindfulness meditation is premised on sustaining non-judgmental awareness of all sensory, cognitive, and self-referential events. The present study combined fMRI, pain-evoking heat, and meditation to identify if mindful-based pain modulation is associated with modifying nociceptive and appraisal processes. Study power calculation analyses employing a sample of forty participants successfully predicted the large behavioral and neural effect sizes. Importantly, we demonstrate that mindfulness meditation directly attenuated self-reported pain (Figure 4) and corresponding brain mechanisms supporting nociception and self-referential processing (Figure 5, 7– 9).

Mindfulness-based pain-relief was moderated by weaker functional connectivity between the contralateral thalamus and the precuneus (Figure 7). The precuneus and thalamus are critically implicated in the quality of awareness of self and sensory environment (i.e., self-consciousness) via connections to brainstem arousal systems [5; 43]. Precuneual and thalamic and thalamus predict loss and CBF increases signal recovery of consciousness, respectively [14; 43; 47]. Together, the precuneus and thalamus form a binding site to integrate to facilitate multisensory integration with internal representations of self [5; 31; 43]. Yet, the precuneus is not directly connected to sensory, ventroposterior lateral thalamus, but rather the anterior-central intralaminar complex and pulvinar nuclei of the thalamus [8]. As the central node of the default mode network, the neural network facilitating self-referential processes, the precuneus exhibits the highest metabolic consumption in the brain [19] and is anatomically situated to integrate somatosensory representations with the sense of self [34; 49]. Higher precuneaul activation is associated with lower pain sensitivity [4; 25] and higher dispositional mindfulness [54]. Thus, the relationship between mindfulness-induced pain relief and weaker thalamic-precuneual connectivity may reflect volitionally mediated disengagement from self-referential appraisals of nociceptive input [5; 43], a potentially novel pain modulatory mechanism.

The present findings also extend upon previous work to demonstrate that mindfulness engages multiple mechanisms to reduce pain. When compared to the controls, mindfulness meditation significantly reduced noxious heat-driven activation in the dACC, SMA, bilateral SII/parietal operculum and posterior insula (Figure 5). The whole-brain regression analysis found that greater meditation-induced pain reductions were associated with greater vmPFC deactivation, a cortical midline structure critically involved in facilitating the experience of a “multifaceted self” [18]. Specifically, the vmPFC is a regulator of self-narrative processing of moment-to-moment experience [5; 22; 31; 37]. Subcortical-vmPFC connections facilitate affect generation of incoming sensory information to produce value-based self-representations [30; 32; 37], the sense of “self and body-ownership”(i.e., “mine-

ness"), and personal significance [5; 22; 32]. It is suitable, then, that mindfulness meditation reduced amygdalar and hippocampal activation during noxious heat, mechanisms that suggest a reduction in affective reactivity to ongoing sensory input [42]. Mindfulness meditation is premised on "letting go and acceptance of accepting arising sensory and cognitive events" and may lower pain by reducing the subjective embodiment of noxious sensations [13]. Thus, these data indicate that mindfulness meditation weakens cortical self-referential midline processing of ascending nociceptive inputs to promote a sensory-egocentric decoupling mechanism.

Although not implicative of direct connectivity, seed-to-seed PPI analyses found that mindfulness meditation induced pain reductions were also associated with weaker functional connectivity between the right OFC – and the contralateral thalamus (Figure 8). As predicted, pain-relief produced by mindfulness meditation was associated with greater decoupling between the contralateral thalamus and the left SI corresponding to the stimulation site (right calf). Thus, we provide novel supplementary evidence that mindfulness meditation reduces pain by attenuating low-level afferent processing to diminish the elaboration of nociception throughout the cortex. The OFC-whole brain PPI analysis provided novel insight to how mindfulness meditation may uniquely uncouple *interpretive* appraisals of sensory, albeit noxious experience. Weaker PFC connectivity with brain mechanisms that are critical for sensory pain discrimination (contralateral posterior insula, SII, and parietal operculum; Figure 9) were associated with greater mindfulness meditation-based pain relief. Lateral OFC projections to the dorsomedial - ventroanterior thalamus [28] drive self-appraisals of low-level sensory input [20; 27; 29]. Thus, we propose that mindfulness-based attention inhibits the integration of self-referential and nociceptive processes through a PFC-nociceptive gating mechanism [17; 44] that may be reflective of a non-evaluative cognitive stance.

As previously described in contemporary and traditional text [6; 23; 35], mindfulness meditation may reduce pain by *uncoupling* egocentric appraisals of salient nociceptive inputs. Converging lines of evidence demonstrate that stronger thalamic-PCC/precuneus connectivity drives chronic pain symptomology [4; 41; 42] and corresponding affective dysregulation [25]. Thus, the enduring chronic pain relief reported in response to mindfulness-based pain therapies [16; 38] may reverse such aberrant signaling. These neurobiological findings are remarkably consistent with the central tenets of mindfulness ("*non/not-self*"; Pali: *Anatta*) to foster a non-reactive sense of self to alleviate suffering [35]. We suggest that mindfulness-based pain relief, after brief mental training, can significantly uncouple self-referential from nociceptive processes, an important finding for the millions of individuals seeking a fast-acting and non-pharmacologic pain treatment.

Supplementary Material

Refer to Web version on PubMed Central for supplementary material.

ACKNOWLEDGMENTS

This work was supported by the National Center for Complementary and Integrative Health (K99/R00-AT008238; R01-AT009693; R21-AT010352; UC San Diego T. Denny Sanford Institute for Empathy and Compassion).

REFERENCES

[1]. Adler-Neal AL, Waugh CE, Garland EL, Shaltout HA, Diz DI, Zeidan F. The Role of Heart Rate Variability in Mindfulness-Based Pain Relief. J Pain 2020;21(3–4):306–323. [PubMed: 31377215]

[2]. Akselrod M, Martuzzi R, Serino A, van der Zwaag W, Gassert R, Blanke O. Anatomical and functional properties of the foot and leg representation in areas 3b, 1 and 2 of primary somatosensory cortex in humans: A 7T fMRI study. Neuroimage 2017;159:473–487. [PubMed: 28629975]

[3]. Baliki MN, Geha PY, Apkarian AV, Chialvo DR. Beyond feeling: chronic pain hurts the brain, disrupting the default-mode network dynamics. J Neurosci 2008;28(6):1398–1403. [PubMed: 18256259]

[4]. Baliki MN, Mansour AR, Baria AT, Apkarian AV. Functional reorganization of the default mode network across chronic pain conditions. PLoS One 2014;9(9):e106133. [PubMed: 25180885]

[5]. Blanke O, Slater M, Serino A. Behavioral, Neural, and Computational Principles of Bodily Self-Consciousness. Neuron 2015;88(1):145–166. [PubMed: 26447578]

[6]. Bohdi B In the Buddha's Words: An Anthology of Discourses from the Pali Canon. Boston, MA: Wisdom Publications, 2005.

[7]. Burrowes SAB, Goloubeva O, Stafford K, McArdle PF, Goyal M, Peterlin BL, Haythornthwaite JA, Seminowicz DA. Enhanced mindfulness-based stress reduction in episodic migraine-effects on sleep quality, anxiety, stress, and depression: a secondary analysis of a randomized clinical trial. Pain 2021.

[8]. Cavada C, Goldman-Rakic PS. Posterior parietal cortex in rhesus monkey: I. Parcellation of areas based on distinctive limbic and sensory corticocortical connections. J Comp Neurol 1989;287(4):393–421. [PubMed: 2477405]

[9]. Cherkin DC, Sherman KJ, Balderson BH, Cook AJ, Anderson ML, Hawkes RJ, Hansen KE, Turner JA. Effect of Mindfulness-Based Stress Reduction vs Cognitive Behavioral Therapy or Usual Care on Back Pain and Functional Limitations in Adults With Chronic Low Back Pain: A Randomized Clinical Trial. JAMA 2016;315(12):1240–1249. [PubMed: 27002445]

[10]. Creswell JD, Taren AA, Lindsay EK, Greco CM, Gianaros PJ, Fairgrieve A, Marsland AL, Brown KW, Way BM, Rosen RK, Ferris JL. Alterations in Resting-State Functional Connectivity Link Mindfulness Meditation With Reduced Interleukin-6: A Randomized Controlled Trial. Biol Psychiatry 2016;80(1):53–61. [PubMed: 27021514]

[11]. Dadi K, Varoquaux G, Machlouzarides-Shalit A, Gorgolewski KJ, Wassermann D, Thirion B, Mensch A. Fine-grain atlases of functional modes for fMRI analysis. Neuroimage 2020;221:117126. [PubMed: 32673748]

[12]. Eklund A, Nichols TE, Knutsson H. Cluster failure: Why fMRI inferences for spatial extent have inflated false-positive rates. Proceedings of the national academy of sciences 2016;113(28):7900–7905.

[13]. Farb NA, Segal ZV, Mayberg H, Bean J, McKeon D, Fatima Z, Anderson AK. Attending to the present: mindfulness meditation reveals distinct neural modes of self-reference. Social Cognitive and Affective Neuroscience 2007;2(4):313–322. [PubMed: 18985137]

[14]. Fiset P, Paus T, Daloze T, Plourde G, Meuret P, Bonhomme V, Hajj-Ali N, Backman SB, Evans AC. Brain mechanisms of propofol-induced loss of consciousness in humans: a positron emission tomographic study. J Neurosci 1999;19(13):5506–5513. [PubMed: 10377359]

[15]. Garland EL, Hanley AW, Nakamura Y, Barrett JW, Baker AK, Reese SE, Riquino MR, Froeliger B, Donaldson GW. Mindfulness-Oriented Recovery Enhancement vs Supportive Group Therapy for Co-occurring Opioid Misuse and Chronic Pain in Primary Care: A Randomized Clinical Trial. JAMA Intern Med 2022.

[16]. Garland EL, Manusov EG, Froeliger B, Kelly A, Williams JM, Howard MO. Mindfulness-oriented recovery enhancement for chronic pain and prescription opioid misuse: results from an early-stage randomized controlled trial. J Consult Clin Psychol 2014;82(3):448–459. [PubMed: 24491075]

[17]. Grant JA, Courtemanche J, Rainville P. A non-elaborative mental stance and decoupling of executive and pain-related cortices predicts low pain sensitivity in Zen meditators. Pain 2011;152(1):150–156. [PubMed: 21055874]

[18]. Gusnard DA, Akbudak E, Shulman GL, Raichle ME. Medial prefrontal cortex and self-referential mental activity: relation to a default mode of brain function. Proc Natl Acad Sci U S A 2001;98(7):4259–4264. [PubMed: 11259662]

[19]. Gusnard DA, Raichle ME. Searching for a baseline: functional imaging and the resting human brain. Nat Rev Neurosci 2001;2(10):685–694. [PubMed: 11584306]

[20]. Halassa MM, Kastner S. Thalamic functions in distributed cognitive control. Nat Neurosci 2017;20(12):1669–1679. [PubMed: 29184210]

[21]. Harrison R, Zeidan F, Kitsaras G, Ozcelik D, Salomons TV. Trait Mindfulness Is Associated With Lower Pain Reactivity and Connectivity of the Default Mode Network. J Pain 2019;20(6):645–654. [PubMed: 30496832]

[22]. Johnson SC, Baxter LC, Wilder LS, Pipe JG, Heiserman JE, Prigatano GP. Neural correlates of self-reflection. Brain 2002;125(Pt 8):1808–1814. [PubMed: 12135971]

[23]. Kabat-Zinn J An outpatient program in behavioral medicine for chronic pain patients based on the practice of mindfulness meditation: theoretical considerations and preliminary results. General Hospital Psychiatry 1982;4(1):33–47. [PubMed: 7042457]

[24]. Kucyi A, Moayedi M, Weissman-Fogel I, Goldberg MB, Freeman BV, Tenenbaum HC, Davis KD. Enhanced medial prefrontal-default mode network functional connectivity in chronic pain and its association with pain rumination. J Neurosci 2014;34(11):3969–3975. [PubMed: 24623774]

[25]. Lee J, Protsenko E, Lazaridou A, Franceschelli O, Ellingsen DM, Mawla I, Isenburg K, Berry MP, Galenkamp L, Loggia ML, Wasan AD, Edwards RR, Napadow V. Encoding of Self-Referential Pain Catastrophizing in the Posterior Cingulate Cortex in Fibromyalgia. Arthritis Rheumatol 2018.

[26]. May LM, Kosek P, Zeidan F, Berkman ET. Enhancement of Meditation Analgesia by Opioid Antagonist in Experienced Meditators. Psychosom Med 2018.

[27]. Montague PR, Berns GS. Neural economics and the biological substrates of valuation. Neuron 2002;36(2):265–284. [PubMed: 12383781]

[28]. Murphy MJM, Deutch AY. Organization of afferents to the orbitofrontal cortex in the rat. J Comp Neurol 2018;526(9):1498–1526. [PubMed: 29524205]

[29]. Nakajima M, Schmitt LI, Halassa MM. Prefrontal Cortex Regulates Sensory Filtering through a Basal Ganglia-to-Thalamus Pathway. Neuron 2019;103(3):445–458.e410. [PubMed: 31202541]

[30]. Northoff G Self and brain: what is self-related processing? Trends Cogn Sci 2011;15(5):186–187; author reply 187–188. [PubMed: 21458358]

[31]. Northoff G, Bermpohl F. Cortical midline structures and the self. Trends in Cognitive Sciences 2004;8(3):102–107. [PubMed: 15301749]

[32]. Northoff G, Heinzel A, de Greck M, Bermpohl F, Dobrowolny H, Panksepp J. Self-referential processing in our brain--a meta-analysis of imaging studies on the self. Neuroimage 2006;31(1):440–457. [PubMed: 16466680]

[33]. O'Reilly JX, Woolrich MW, Behrens TE, Smith SM, Johansen-Berg H. Tools of the trade: psychophysiological interactions and functional connectivity. Soc Cogn Affect Neurosci 2012;7(5):604–609. [PubMed: 22569188]

[34]. Penfield W, Boldrey E. Somatic motor and sensory representation in the cerebral cortex of man as studied by electrical stimulation. Brain 1937;60:389.

[35]. Phra T The Buddha's doctrine of anattā. Bangkok, Thailand: Dhamma Study & Practice Group, 1990.

[36]. Raichle ME. The brain's default mode network. Annu Rev Neurosci 2015;38:433–447. [PubMed: 25938726]

[37]. Roy M, Shohamy D, Wager TD. Ventromedial prefrontal-subcortical systems and the generation of affective meaning. Trends Cogn Sci 2012;16(3):147–156. [PubMed: 22310704]

[38]. Seminowicz DA, Burrowes SAB, Kearson A, Zhang J, Krimmel SR, Samawi L, Furman AJ, Keaser ML, Gould NF, Magyari T, White L, Goloubeva O, Goyal M, Peterlin BL,

Haythornthwaite JA. Enhanced mindfulness-based stress reduction in episodic migraine: a randomized clinical trial with magnetic resonance imaging outcomes. Pain 2020;161(8):1837–1846. [PubMed: 32701843]

[39]. Sheline YI, Barch DM, Price JL, Rundle MM, Vaishnavi SN, Snyder AZ, Mintun MA, Wang S, Coalson RS, Raichle ME. The default mode network and self-referential processes in depression. Proc Natl Acad Sci U S A 2009;106(6):1942–1947. [PubMed: 19171889]

[40]. Smith SM, Nichols TE. Threshold-free cluster enhancement: addressing problems of smoothing, threshold dependence and localisation in cluster inference. Neuroimage 2009;44(1):83–98. [PubMed: 18501637]

[41]. Tu Y, Fu Z, Mao C, Falahpour M, Gollub RL, Park J, Wilson G, Napadow V, Gerber J, Chan ST, Edwards RR, Kaptchuk TJ, Liu T, Calhoun V, Rosen B, Kong J. Distinct thalamocortical network dynamics are associated with the pathophysiology of chronic low back pain. Nat Commun 2020;11(1):3948. [PubMed: 32769984]

[42]. Vachon-Presseau E, Tetreault P, Petre B, Huang L, Berger SE, Torbey S, Baria AT, Mansour AR, Hashmi JA, Griffith JW, Comasco E, Schnitzer TJ, Baliki MN, Apkarian AV. Corticolimbic anatomical characteristics predetermine risk for chronic pain. Brain 2016;139(Pt 7):1958–1970. [PubMed: 27190016]

[43]. Vanhaudenhuyse A, Noirhomme Q, Tshibanda LJ, Bruno MA, Boveroux P, Schnakers C, Soddu A, Perlbarg V, Ledoux D, Brichant JF, Moonen G, Maquet P, Greicius MD, Laureys S, Boly M. Default network connectivity reflects the level of consciousness in non-communicative brain-damaged patients. Brain 2010;133(Pt 1):161–171. [PubMed: 20034928]

[44]. Wager TD, Davidson ML, Hughes BL, Lindquist MA, Ochsner KN. Prefrontal-subcortical pathways mediating successful emotion regulation. Neuron 2008;59(6):1037–1050. [PubMed: 18817740]

[45]. Wells RE, Collier J, Posey G, Morgan A, Auman T, Strittmatter B, Magalhaes R, Adler-Neal A, McHaffie JG, Zeidan F. Attention to breath sensations does not engage endogenous opioids to reduce pain. Pain 2020;161(8):1884–1893. [PubMed: 32701847]

[46]. Worsley KJ, Marrett S, Neelin P, Vandal AC, Friston KJ, Evans AC. A unified statistical approach for determining significant signals in images of cerebral activation. Human brain mapping 1996;4(1):58–73. [PubMed: 20408186]

[47]. Xie G, Deschamps A, Backman SB, Fiset P, Chartrand D, Dagher A, Plourde G. Critical involvement of the thalamus and precuneus during restoration of consciousness with physostigmine in humans during propofol anaesthesia: a positron emission tomography study. Br J Anaesth 2011;106(4):548–557. [PubMed: 21285081]

[48]. Yarnitsky D, Sprecher E, Zaslansky R, Hemli JA. Multiple session experimental pain measurement. Pain 1996;67(2–3):327–333. [PubMed: 8951926]

[49]. Zeharia N, Hofstetter S, Flash T, Amedi A. A Whole-Body Sensory-Motor Gradient is Revealed in the Medial Wall of the Parietal Lobe. J Neurosci 2019;39(40):7882–7892. [PubMed: 31405923]

[50]. Zeidan F, Adler-Neal AL, Wells RE, Stagnaro E, May LM, Eisenach JC, McHaffie JG, Coghill RC. Mindfulness-Meditation-Based Pain Relief Is Not Mediated by Endogenous Opioids. J Neurosci 2016;36(11):3391–3397. [PubMed: 26985045]

[51]. Zeidan F, Emerson NM, Farris SR, Ray JN, Jung Y, McHaffie JG, Coghill RC. Mindfulness Meditation-Based Pain Relief Employs Different Neural Mechanisms Than Placebo and Sham Mindfulness Meditation-Induced Analgesia. J Neurosci 2015;35(46):15307–15325. [PubMed: 26586819]

[52]. Zeidan F, Martucci KT, Kraft RA, Gordon NS, McHaffie JG, Coghill RC. Brain mechanisms supporting the modulation of pain by mindfulness meditation. J Neurosci 2011;31(14):5540–5548. [PubMed: 21471390]

[53]. Zeidan F, Martucci KT, Kraft RA, McHaffie JG, Coghill RC. Neural correlates of mindfulness meditation-related anxiety relief. Soc Cogn Affect Neurosci 2014;9(6):751–759. [PubMed: 23615765]

[54]. Zeidan F, Salomons T, Farris SR, Emerson NM, Adler-Neal A, Jung Y, Coghill RC. Neural mechanisms supporting the relationship between dispositional mindfulness and pain. Pain 2018;159(12):2477–2485. [PubMed: 30015711]

[55]. Zeidan F, Salomons T, Farris SR, Emerson NM, Neal AA, Jung Y, Coghill RC. Neural Mechanisms Supporting the Relationship between Dispositional Mindfulness and Pain. Pain 2018.

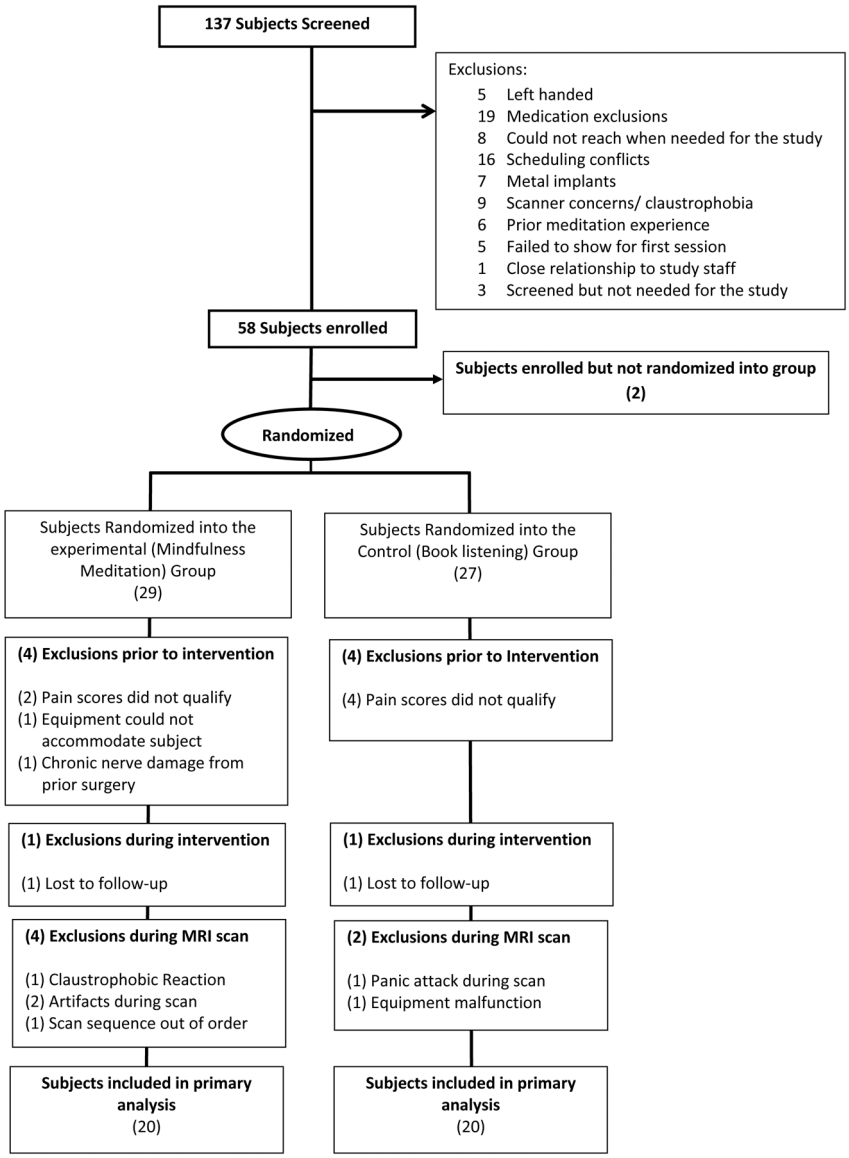

Figure 1:

Consolidated Standards of Reporting Trials (CONSORT) flow diagram: At screening, 79 participants were excluded for not meeting inclusion-exclusion criteria. Fifty-eight participants were enrolled into the study. After session 1, participants were dropped for low pain sensitivity (n=6), equipment not fitting (n=1), and chronic pain (n=1). After randomization, a subject from each group was dismissed for “no-shows”. In the MRI session, a total of four participants from the mindfulness group and 2 from the control group were dismissed for several reasons. Two participants completed their respective fMRI scans but were removed from the final analysis (and replaced at random) due to a procedural error and an exhibited fMRI related artifact, respectively. The targeted sample size of forty participants were included in the study.

Figure 2:

Study procedures: Session 1: After attaining informed consent, participants were trained to use pain intensity and unpleasantness visual analog scale (VAS) in response to noxious heat stimulation (psychophysical training). The experimental Heat series included ten, 10 second plateaus of 49°C interleaved with 14 seconds 35°C stimulation applied to the back of the right calf. Participants were instructed to keep their eyes closed and rest in response to, two heat series. VAS ratings were collected after each respective heat series. After two heat series, participants were instructed to "sit quietly for 10 minutes" to control for the time spent initiating meditation in Session 6. After this 10-minute period, participants were administered two more heat series and VAS ratings were collected afterward. Participants were then randomized to a four-session (20 minutes/session) mindfulness meditation or a control group that listened to the *Natural History of Selborne* across four, 20 minutes sessions. After successful completion of their respective regimens (Session 2–5), participants reported to the MRI center for post-intervention functional MRI sessions. Session 6: After being positioned in the scanner, we administered two Heat series while participants rested with their eyes closed during fMRI acquisition. VAS ratings were collected after each respective heat series. Before anatomical acquisition, we instructed the members of the mindfulness group to "begin meditating and to continue until the end of the experiment." The control group was instructed to "keep eyes closed". After 10 minutes elapsed, we administered two more Heat series during functional acquisition and collected pain ratings after each respective series.

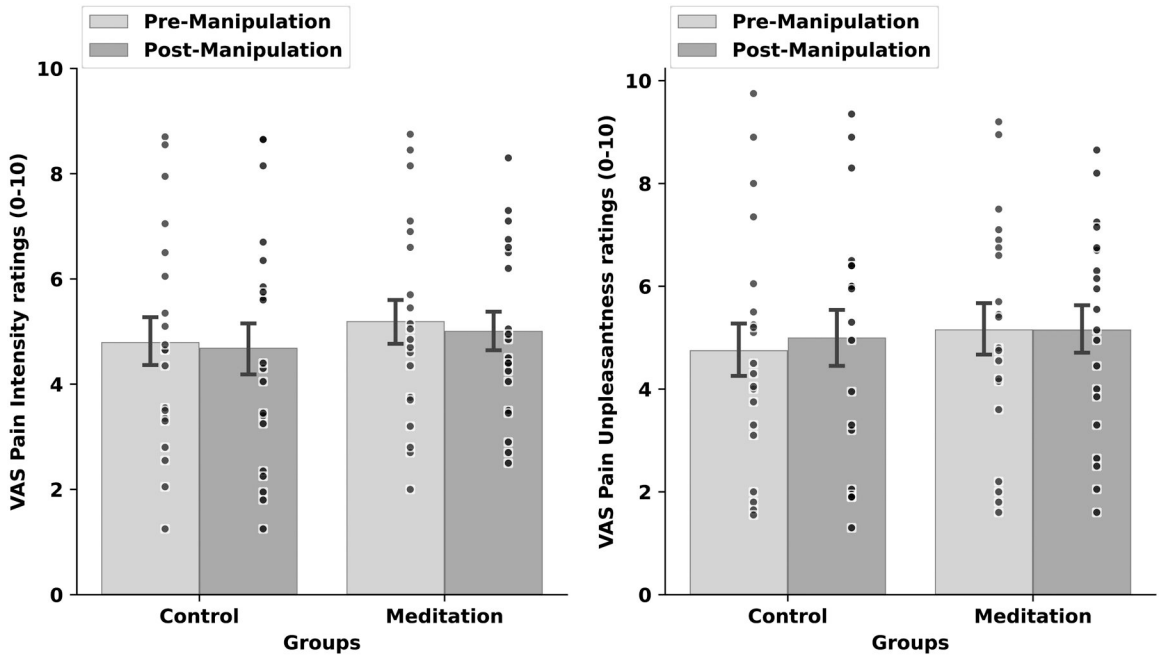

Figure 3:

Psychophysical visual analog scale (VAS) pain intensity (left) and unpleasantness (right) ratings (± 1 standard error of the mean) in response to pre-manipulation (rest) vs. post-manipulation (rest) and noxious heat (49°C) during the pre-intervention psychophysical testing session. There were no significant within or between group effects.

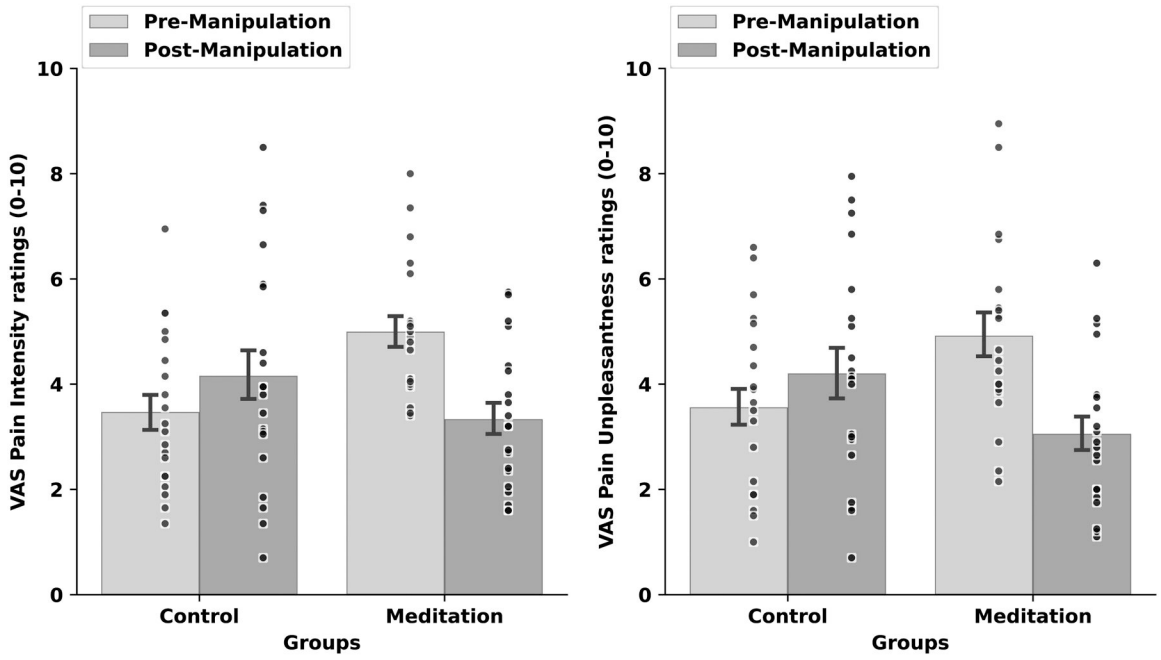

Figure 4:

Psychophysical visual analog scale (VAS) pain intensity (left) and unpleasantness (right) ratings (± 1 standard error of the mean) in response to pre-manipulation (rest) vs. post-manipulation (rest; meditation) and noxious heat (49°C) during the post-intervention MRI session. Mindfulness meditation produced significant reductions in pain intensity (−32%) and pain unpleasantness (−33%) ratings when compared to rest and the change in pain from pre to post-manipulation in the control group (ps<.001).

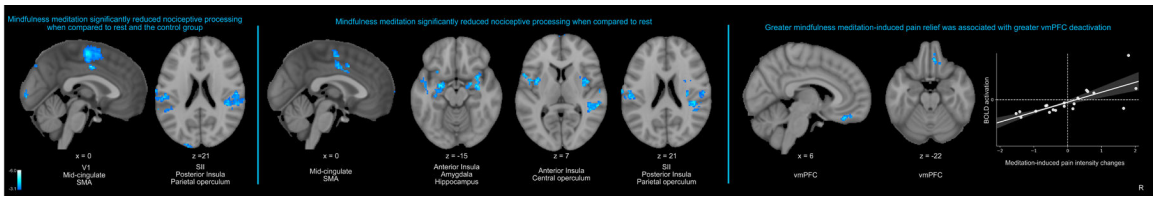

Figure 5:

All neuroimaging analyses were performed during noxious heat (49°C > 35°C). Left panel: The whole-brain independent samples t-test revealed that mindfulness meditation significantly reduced activation in the bilateral posterior insula, secondary somatosensory cortices (SII), parietal operculum, dorsal ACC (dACC), supplementary motor area (SMA), and primary visual cortex (V1) during noxious heat when compared to rest and the change in pain from pre to post-manipulation in the control group. Middle panel: A paired-samples t-test employing a change in pain (demeaned post-manipulation – pre- manipulation) found that meditation produced significant reductions in the dACC, SMA, bilateral anterior/posterior insula, amygdala, hippocampus, central-parietal operculum and SII when compared to rest. Right panel: Greater mindfulness-based pain intensity reductions, from rest to meditation, was associated with stronger vmPFC deactivation (r=.73, p<.001). R, subject right, slice locations correspond to standard stereotaxic space.

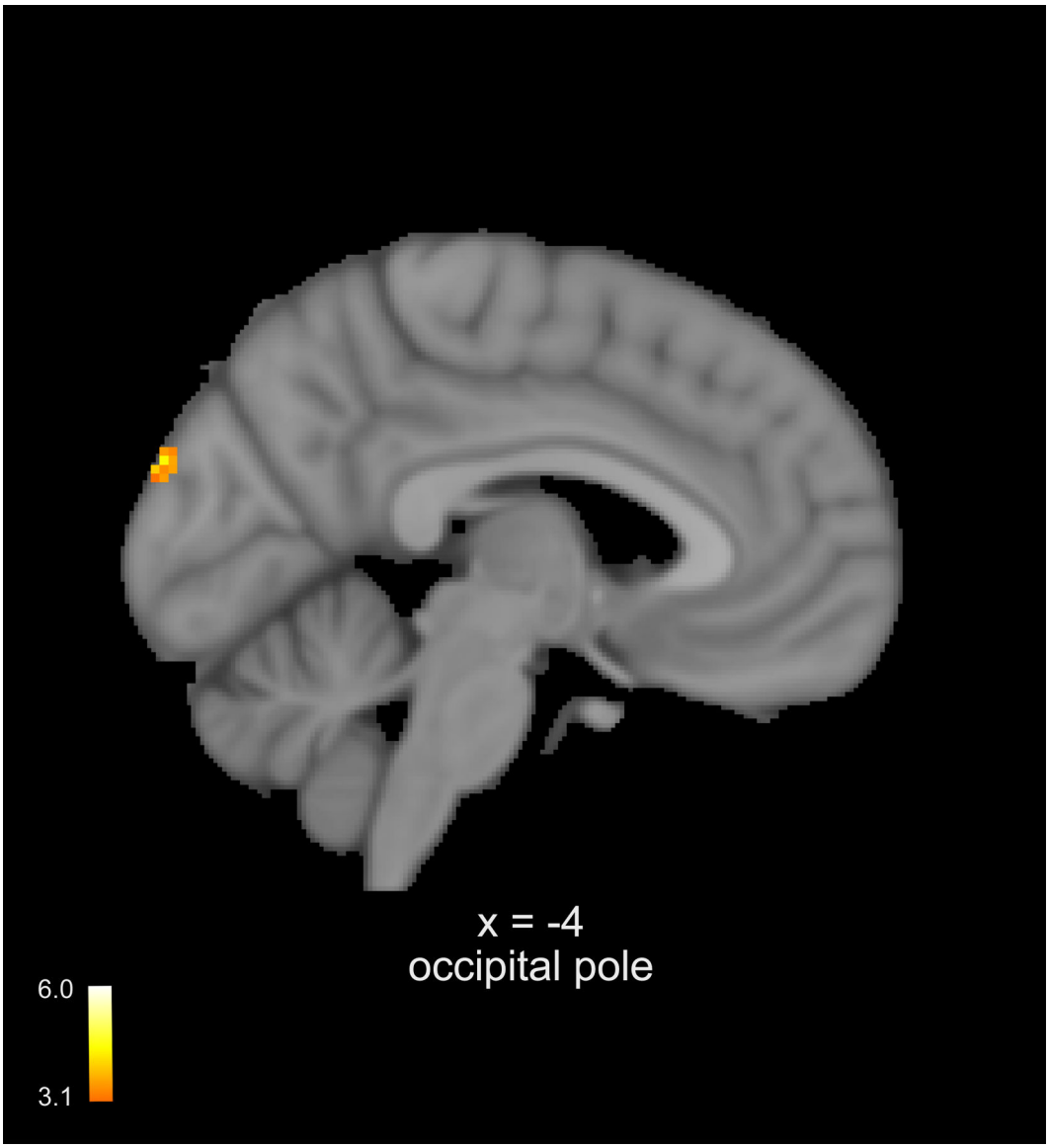

Figure 6:

Neuroimaging analyses were performed during noxious heat (49°C > 35°C). A paired-samples t-test employing a change in pain (demeaned post-manipulation – pre-manipulation) found that the controls exhibited a significant increase in occipital lobe activation in the second half of the scan when compared to the first half of the scans. Slice locations correspond to standard stereotaxic space.

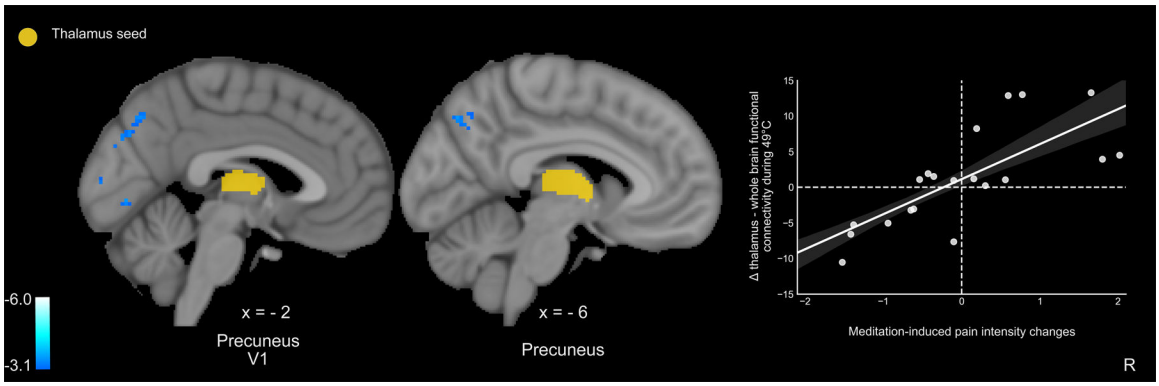

Figure 7:

Left thalamic-whole brain psychophysiological interaction analyses (PPI; z = ± 3.1, p < .05) were performed during 49°C plateaus. PPI analyses were conducted during meditation as compared to rest. Pain intensity and unpleasantness ratings were regressed on the mean effect, respectively. Greater mindfulness meditation-induced pain intensity relief was moderated by weaker thalamic connectivity with the precuneus and primary visual cortex (V1) (r=.74, *p*<.001). R, subject right, slice locations correspond to standard stereotaxic space.

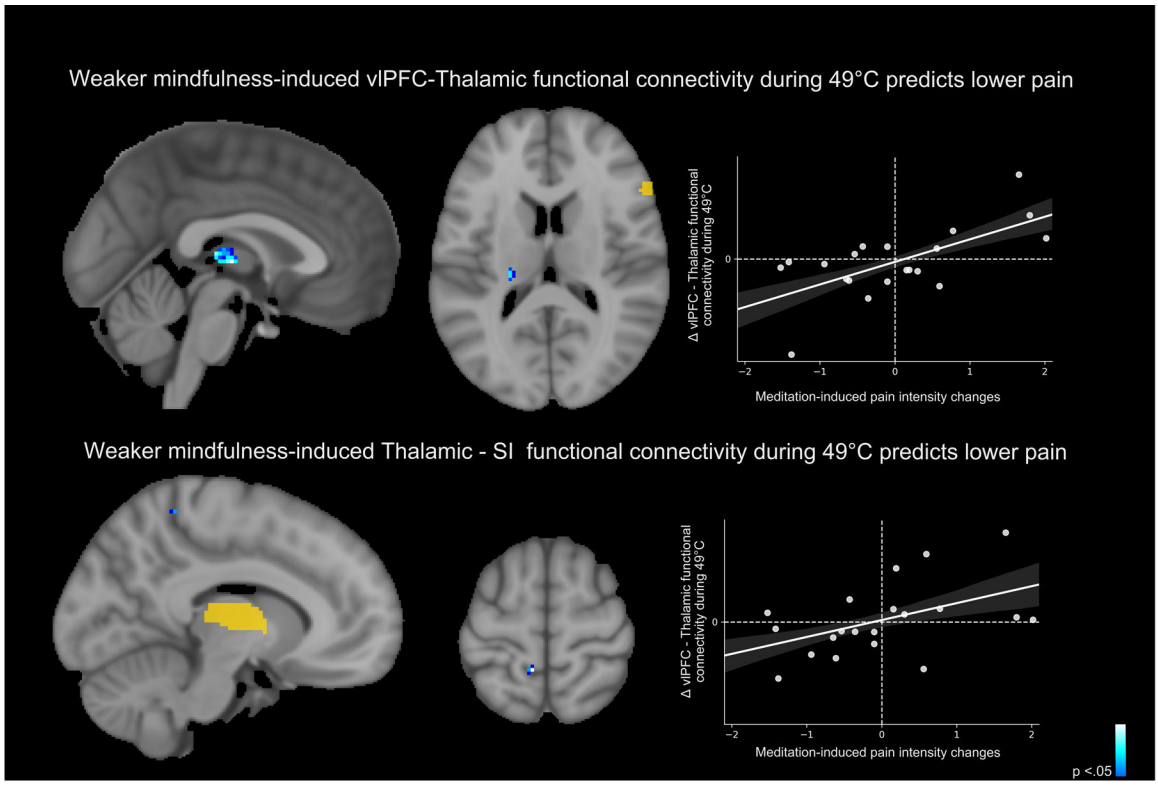

Figure 8:

Separate seed-to-seed psychophysiological interaction analyses (PPI) were conducted (Threshold-Free Cluster Enhancement, $p < .05$) [40] to determine if a) right orbitofrontal cortical (OFC) connectivity with the left thalamus and b) left thalamus with the primary somatosensory cortex (SI) predicted mindfulness meditation-induced pain relief, respectively. Top panel: Weaker right OFC connectivity with the contralateral thalamus predicted mindfulness-induced pain reductions from rest to meditation ($r = .65$, $p = .001$). Bottom panel: Weaker thalamic-SI functional connectivity predicted stronger meditation-induced pain intensity reductions ($r = .48$, $p = .03$). There were no other significant effects for either group. R, subject right, slice locations correspond to standard stereotaxic space.

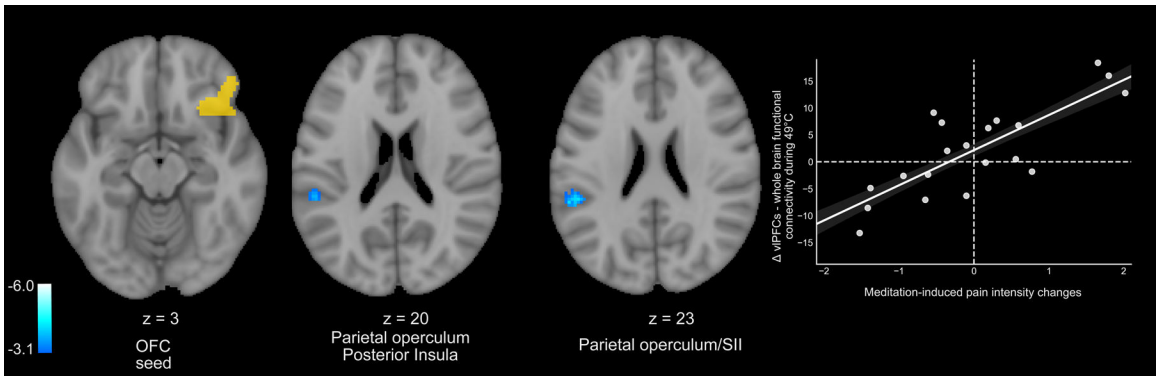

Figure 9:

Right orbitofrontal cortex (OFC) – whole-brain psychophysiological interaction analyses (PPI) were performed during 49°C plateaus. PPI analyses ($z = \pm 3.1$, $p < .05$) were conducted during meditation as compared to rest. Pain intensity and unpleasantness ratings were regressed on the mean effect, respectively. Greater mindfulness meditation-induced pain intensity reductions from rest to meditation was moderated by weaker right OFC connectivity with the contralateral posterior insula, SII, and parietal operculum ($r = .80$, $p < .001$). There were no other significant meditation-related mean effects, correlations, or control group effects. R, subject right, slice locations correspond to standard stereotaxic space.

Table 1.

Brain coordinates on significant activation and deactivations

region	Z score	P value	(x, y, z)
Figure 5**: Meditation (rest vs. meditation) < Controls (pre vs. post rest)**			
bilateral occipital pole	4.87	7.77×10^{-11}	−52, −84, −8
bilateral supplementary motor area, bilateral dorsal anterior cingulate cortex	5.08	2.22×10^{-14}	−4, −8, 40
left secondary somatosensory cortex	4.65	1.52×10^{-4}	−60, −24, 10
left posterior insula	4.05	1.68×10^{-4}	−50, −46, 24
right parietal operculum	5.12	5.96×10^{-8}	44, −34, 22
Figure 5**: mindfulness group: rest > meditation**			
bilateral supplementary motor area, bilateral dorsal anterior cingulate cortex	5.34	9.47×10^{-9}	−2, −10, 54
left anterior insula, left amygdala, left hippocampus	4.82	2.17×10^{-11}	−24, −12, −14
right anterior insula, right amygdala, right hippocampus	4.91	3.16×10^{-6}	34, −8, −16
right central operculum, right parietal operculum	4.83	2.90×10^{-8}	48, −44, 16
left posterior insula, left secondary somatosensory cortex	4.61	4.14×10^{-9}	−54, −20, 22
Figure 5**: mindfulness group: meditation – rest and brain correlates of pain intensity reductions**			
right ventromedial prefrontal cortex	4.42	0.0418	8, 36, −22
Figure 6**: control group: Post scan rest > pre scan rest**			
Left occipital lobe			− 4, ,
Figure 7**: mindfulness group: meditation – rest thalamic decoupling correlates of pain intensity reductions**			
precuneus	3.94	8.18×10^{-5}	8, −72, 30
occipital pole	4.02	0.0209	0, −78, −2
Figure 8**: mindfulness group: meditation – rest seed-seed connectivity correlates of pain intensity reductions**			
thalamus	*	0.0164	0, −16, 4
left primary somatosensory cortex	*	0.0313	−8, −44, 62
Figure 9**: mindfulness group: meditation – rest vlPFC connectivity correlates of pain intensity reductions**			
left parietal operculum, left posterior insula, left secondary somatosensory cortex	4.22	0.0499	−50, −38, 24

Table 2.

Mean [standard deviation (SD)] of the parameter estimates extracted from significant brain deactivation (Figure 5 left panel) during noxious heat for pre – and post-manipulation for the mindfulness meditation (Meditation) and book-listening (Control) group, respectively.

	Meditation group		Control group	
	Pre manipulation	**Post manipulation**	**Pre manipulation**	**Post manipulation**
Mean (SD)	0.21 (0.19)	0.04 (0.11)	0.19 (0.18)	0.22 (0.23)